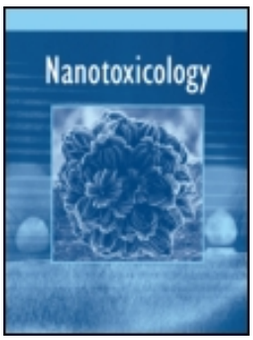

Nanotoxicology

ISSN: 1743-5390 (Print) 1743-5404 (Online) Journal homepage: http://www.tandfonline.com/loi/inan20

Coating-dependent induction of cytotoxicity and genotoxicity of iron oxide nanoparticles

Zuzana Magdolenova, Martina Drlickova, Kristi Henjum, Elise Rundén-Pran, Jana Tulinska, Dagmar Bilanicova, Giulio Pojana, Alena Kazimirova, Magdalena Barancokova, Miroslava Kuricova, Aurelia Liskova, Marta Staruchova, Fedor Ciampor, Ivo Vavra, Yolanda Lorenzo, Andrew Collins, Alessandra Rinna, Lise Fjellsbø, Katarina Volkovova, Antonio Marcomini, Mahmood Amiry-Moghaddam & Maria Dusinska

To cite this article: Zuzana Magdolenova, Martina Drlickova, Kristi Henjum, Elise Rundén-Pran, Jana Tulinska, Dagmar Bilanicova, Giulio Pojana, Alena Kazimirova, Magdalena Barancokova, Miroslava Kuricova, Aurelia Liskova, Marta Staruchova, Fedor Ciampor, Ivo Vavra, Yolanda Lorenzo, Andrew Collins, Alessandra Rinna, Lise Fjellsbø, Katarina Volkovova, Antonio Marcomini, Mahmood Amiry-Moghaddam & Maria Dusinska (2015) Coating-dependent induction of cytotoxicity and genotoxicity of iron oxide nanoparticles, Nanotoxicology, 9:sup1, 44-56, DOI: 10.3109/17435390.2013.847505

To link to this article: http://dx.doi.org/10.3109/17435390.2013.847505

http://informahealthcare.com/nan
ISSN: 1743-5390 (print), 1743-5404 (electronic)

Nanotoxicology

Nanotoxicology, 2015; 9(S1): 44–56
 DOI: 10.3109/17435390.2013.847505

informa
healthcare

ORIGINAL ARTICLE

Coating-dependent induction of cytotoxicity and genotoxicity of iron oxide nanoparticles

Zuzana Magdolenova[1,2], Martina Drlickova[3,4], Kristi Henjum[1], Elise Rundén-Pran[1], Jana Tulinska[3], Dagmar Bilanicova[5], Giulio Pojana[5], Alena Kazimirova[3], Magdalena Barancokova[3], Miroslava Kuricova[3], Aurelia Liskova[3], Marta Staruchova[3], Fedor Ciampor[6], Ivo Vavra[6], Yolanda Lorenzo[7], Andrew Collins[7], Alessandra Rinna[1], Lise Fjellsbø[1], Katarina Volkovova[3], Antonio Marcomini[5], Mahmood Amiry-Moghaddam[8], and Maria Dusinska[1]

[1]Health Effects Laboratory, Department of Environmental Chemistry, NILU, Norwegian Institute for Air Research, Kjeller, Norway, [2]Department of Molecular Biology, Faculty of Natural Sciences, Comenius University, Bratislava, Slovakiá, [3]Medical Faculty, Slovak Medical University, Bratislava, Slovakia, [4]Centre for Chemical Substances and Preparations, Bratislava, Slovakia, [5]Department of Environmental Sciences, Informatics and Statistics, University Ca' Foscari Venice, Venice, Italy, [6]Institute of Virology and Institute of Electrical Engineering, Slovak Academy of Sciences, Bratislava, Slovakia, [7]Department of Nutrition, and [8]Department of Anatomy, University of Oslo, Oslo, Norway

Abstract

Surface coatings of nanoparticles (NPs) are known to influence advantageous features of NPs as well as potential toxicity. Iron oxide (Fe_3O_4) NPs are applied for both medical diagnostics and targeted drug delivery. We investigated the potential cytotoxicity and genotoxicity of uncoated iron oxide (U-Fe_3O_4) NPs in comparison with oleate-coated iron oxide (OC-Fe_3O_4) NPs. Testing was performed *in vitro* in human lymphoblastoid TK6 cells and in primary human blood cells. For cytotoxicity testing, relative growth activity, trypan blue exclusion, ^{3}H-thymidine incorporation and cytokinesis-block proliferation index were assessed. Genotoxicity was evaluated by the alkaline comet assay for detection of strand breaks and oxidized purines. Particle characterization was performed in the culture medium. Cellular uptake, morphology and pathology were evaluated by electron microscopy. U-Fe_3O_4 NPs were found not to be cytotoxic (considering interference of NPs with proliferation test) or genotoxic under our experimental conditions. In contrast, OC-Fe_3O_4 NPs were cytotoxic in a dose-dependent manner, and also induced DNA damage, indicating genotoxic potential. Intrinsic properties of sodium oleate were excluded as a cause of the toxic effect. Electron microscopy data were consistent with the cytotoxicity results. Coating clearly changed the behaviour and cellular uptake of the NPs, inducing pathological morphological changes in the cells.

Keywords

Coating, cytotoxicity, DNA damage, genotoxicity, human lymphoblastoid TK6 cells, human peripheral lymphocytes, iron oxide, nanoparticles

History

Received 8 August 2013
Accepted 18 September 2013
Published online 14 November 2013

Introduction

Iron oxide nanoparticles (NPs) are applied within a variety of fields, including medical diagnostics and targeted delivery of therapeutic drugs (Berry et al., 2004; Jain et al., 2008; Kim et al., 2007). The features of the iron oxide (Fe_3O_4) NPs change with introduction of different functional groups to the magnetite NP-core, and thereby novel potential applications are emerging. Manufactured superparamagnetic iron oxide particles with different sizes and surface coatings are used as magnetic resonance (MR) contrast medium with applications ranging from diagnostic imaging to molecular medicine (Schütz et al., 2013a). Large particles (50–150 nm) are used for magnetic resonance imaging (MRI) of the liver and spleen, especially for detecting metastases. Smaller particles (20 nm) show a different organ distribution and have a potential for improving non-invasive lymph node assessment or characterizing vulnerable atherosclerotic plaques (Schütz et al., 2013a). Other applications of small superparamagnetic irone oxide particles include MRI of the bone marrow and determination of perfusion parameters in tumours or other tissues such as myocardium. Iron oxide NPs with a modified coat can be used in so-called molecular imaging, such as receptor-directed imaging, cell labelling for *in vivo* monitoring of cell migration (e.g. stem cells), and labelling of gene constructs in gene therapy. In tumour therapy, Fe_3O_4 NPs can serve as mediators for hyperthermia (Schütz et al., 2013a; Taupitz et al., 2003). Thus, changing the physico-chemical properties of Fe_3O_4 NPs by surface modifications affects biocompatibility (Guardia et al., 2007), cellular uptake (Cengelli et al., 2006) and toxicity (Schütz et al., 2013b) as well as stability, aggregation state and size. The right properties are crucial for biomedical applications, but could also influence potential toxicity. Oleate is widely used as a surfactant in the synthesis of monodispersed magnetic NPs, such as iron oxide, to reduce interparticulate interactions and stabilize the NPs in solution (Yin et al., 2005; Zhang et al., 2006).

Despite the great potential for applications of Fe_3O_4 NPs, there are scant data on their toxic potential (Berry et al., 2004; Schütz et al., 2013b). It has been shown that *in vitro* toxicity depends on surface coating as iron oxide NPs with an added carboxyl group exhibit higher cytotoxicity than NPs with an added amine group

Correspondence: Maria Dusinska, Health Effects Laboratory, Department of Environmental Chemistry, NILU, Norwegian Institute for Air Research, Instituttveien 18, 2027 Kjeller, Norway. Tel: +47 63898157. E-mail: maria.dusinska@nilu.no

(Auffan et al., 2006; Ying & Hwang, 2010). Oleate coating of nickel ferrite NPs has been found to decrease cell viability, compared with uncoated NPs (Yin et al., 2005).

There is also a lack of data related to genotoxic potential of NPs with different coatings. Oleate coated ZnO NPs induced micronuclei whereas uncoated ZnO NPs were found not to be genotoxic (Yin et al., 2010). Uncoated Fe_3O_4 NPs have been found to increase DNA oxidation (detected as sites sensitive to formamidopyrimidine DNA glycosylase (FPG), using a modified comet assay) in human lung epithelial cells (A549), although DNA strand breaks were not detected (Karlsson et al., 2008, 2009). Fe_3O_4 NPs loaded with daunorubicin (Fe_3O_4-MNPs/DNR) did not induce micronuclei formation in bone marrow of mice following short term injection exposure (Wu et al., 2010).

As the different surface coatings of NPs may influence potential cyto- and genotoxicity, we investigated the effect of uncoated (U-Fe_3O_4) and oleate-coated (OC-Fe_3O_4) iron oxide NPs *in vitro*. Human TK6 lymphoblastoid cells and primary peripheral lymphocytes (isolated from human blood) were tested with both cytotoxicity and genotoxicity assays. Uptake of the NPs as well as morphological cellular changes were investigated by transmission electron microscopy (TEM). The cellular models applied represent the blood compartment, which is a highly relevant target for NPs in nanomedicine.

Material and methods

Characterization of NPs

OC-Fe_3O_4 and U-Fe_3O_4 NPs were provided from PlasmaChem (Berlin, D) as aqueous, dark brown dispersions (codes PL-M-Fe_3O_4 and PL-A-Fe_3O_4, respectively), both with nominal size of 8 ± 3 nm and declared concentrations of 7% (as vol., code PL-M-Fe_3O_4) and 3% (as vol., code PL-A-Fe_3O_4), respectively. OC-Fe_3O_4 NPs were declared to contain also ~3% of oleic acid as stabilizer. Despite the name of the coating (oleic acid), we found that the coating was added as sodium oleate, confirmed by the provider. Investigated NPs were characterized by a combination of analytical techniques. Mean average size, shape and crystal structure of primary particles were determined by TEM analysis on a Jeol (Tokyo, Japan) 3010 TEM operating at 300 kV. Surface area and pore volume of U-Fe_3O_4 NPs were obtained by nitrogen adsorption at an adsorption temperature of −196 °C, after gently evaporating the water at room temperature and further heating the sample under high vacuum at 300 °C for 2 h (Brunauer et al., 1938). The magnetic properties have been determined with a Superconducting Quantum Interference Device magnetometer by Quantum Design (San Diego, CA).

Size distributions of dispersed OC-Fe_3O_4 and U-Fe_3O_4 NPs in biological medium were determined as hydrodynamic diameter by Dynamic Light Scattering (DLS) with a Nicomp Submicron Particle SizerAutodilute® Model 370 (Santa Barbara, CA). This instrument can automatically recognize, in the 0.5–6000 nm range, up to three size distributions of particles concurrently present through a patented software algorithm. The actual concentrations of particles in the suspension were determined by Atomic Absorbance Spectroscopy (AAS) after acid digestion of the suspension. Purity of NPs was determined by Inductively Coupled Plasma-Optical Emission Spectroscopy (ICP-OES). Oleic acid content was determined by HPLC-MS. Free cations (Na^+, Ca^{2+}, K^+) in the original OC-Fe_3O_4 suspension were determined by Ion Chromatography (IC). The main physical and chemical properties of selected NPs are summarized in Table 1. The TEM JEOL 1200EX with 120 kV accelerating voltage was used for the characterization (size, size distribution and crystalline phase control) of NPs (Figure 1). The TEM specimens were

Table 1. Main physical and chemical properties of tested iron oxide nanoparticles.

NP code	pH of suspension	TEM Size (nm)	Primary particle morphology (TEM)	Surface area (BET) [m^2/g]	Purity[1]	Particle concentration (mg/mL)[3]	Impurities of toxicological concern	Magnetic behaviour	Z-potential at pH 7 (mV)	Size in RPMI-1640 + 10% FBS (nm)
PL-M-Fe_3O_4 (OC Fe_3O_4)	5.95	5–12	Ellipsoidal particle, octahedral structure, av. Size 10×7 nm	92[2]	>99%	260	Free oleate[4] (960 ppm), Na^{+5} (26.000 ppm)/Ca^{+5} (1.300 ppm)/K^{+5} (730 ppm)	superparamagnetic	−32	39 ± 6, 165 ± 18[6]
PL-A-Fe_3O_4 (U-Fe_3O_4)	2.64	5–13	Ellipsoidal particle, octahedral structure, av. Size 9×7	92	>99%	28	none	paramagnetic	−2.8	1240 ± 780[6]

[1]By ICP-OES. [2]Estimated equal to the uncoated nanomagnetite of U-Fe_3O_4 NPs. [3]By AAS. [4]By HPLC-MS. [5]By IC. [6]DLS intensity-based average sizes in biological medium after 15 min.

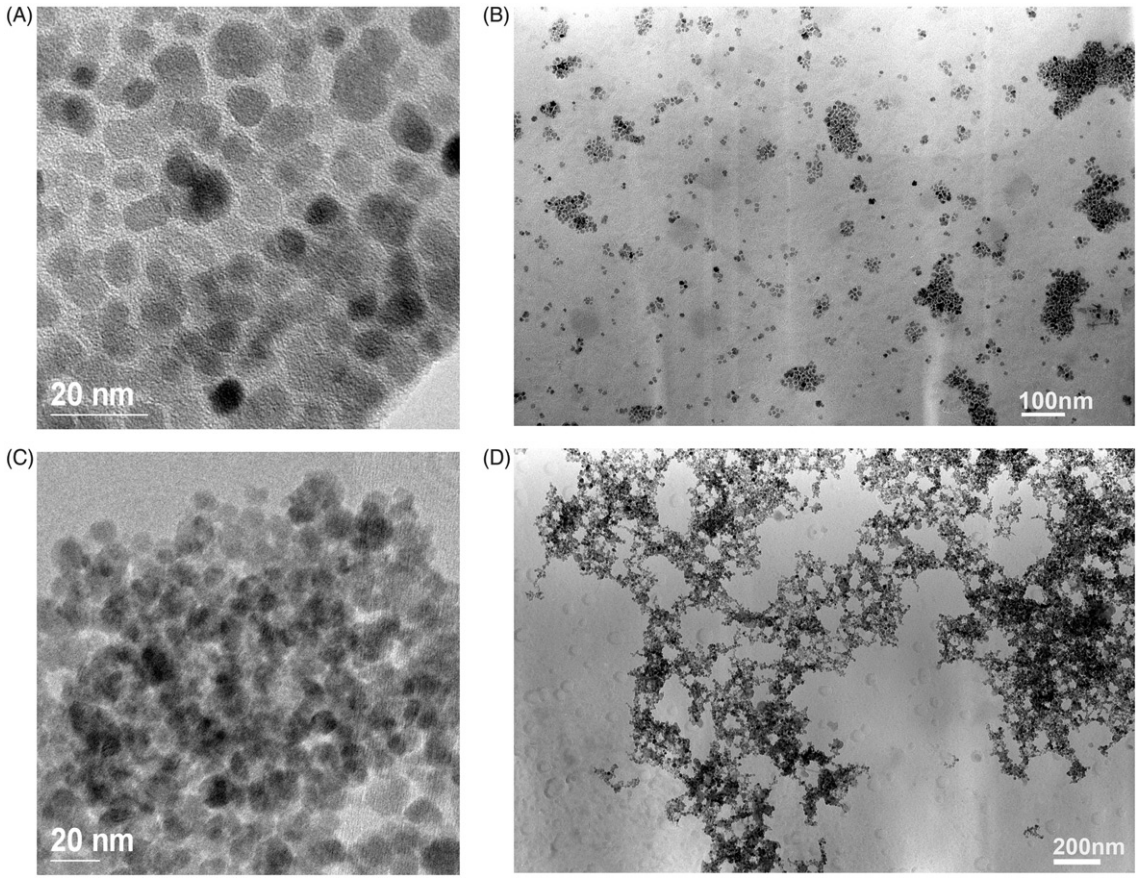

Figure 1. Typical transmission electron microscopy (TEM) images of coated iron oxide nanoparticles (OC-Fe_3O_4 NPs) (A and B) and uncoated iron oxide NPs (U-Fe_3O_4 NPs) (C and D).

prepared by drying of small drop of the nano-colloid on the surface of supporting amorphous carbon foil.

NP dispersion protocols and preparation of sodium oleate

U-Fe_3O_4 NPs and OC-Fe_3O_4 NPs were provided as suspensions in water. A stock solution was prepared fresh prior to each experiment by dilution in PBS to obtain a final concentration of 2 mg/ml iron (dilution 1:10 for U-Fe_3O_4 and dilution 1:94 for OC-Fe_3O_4 NPs). The diluted stock solution of U-Fe_3O_4 can be stored for a few hours at 4 °C or room temperature, while for OC-Fe_3O_4 NPs the stock solution can be stored for several weeks at 4 °C. Immediately before use aliquots were vortexed for 1 min and serial dilutions in the cell culture medium were made to obtain the full range (0.12–75 μg/cm^2) of NP suspension. NP-containing medium was immediately added to the cells.

Sodium oleate (Sigma) was diluted in PBS to a 2.5 mg/ml concentration and further diluted in cell culture medium to obtain concentrations of 10.8, 21.6 and 108 μg/ml which correspond to 1×, 2× and 10× higher concentration than the concentration of sodium oleate present in 75 μg/cm^2 of OC-Fe_3O_4 NPs. Medium containing sodium oleate was mixed with the cells and treated for 24 h (for TBE assay) or 48 h (for RGA assay).

Cell isolation, cultivation and NP exposure

TK6 human lymphoblast cells (obtained from the European Collection of Cell Cultures – ECACC, Cat. No. 95111735) were maintained in RPMI 1640 (Cat. No. R8758, Sigma) culture medium supplemented with 10% (v/v) heat-inactivated foetal bovine serum (FBS), 100 U/ml penicillin and 100 μg/ml streptomycin. Cells were grown in suspension at 37 °C in an atmosphere of 5% CO_2 and 100% humidity, and routinely diluted to $2 \times 10^5 - 1 \times 10^6$ cells/ml. For experiments, TK6 cells were sub-cultured at a density of 4×10^5 cells/ml into 6-well plates with 2 ml of culture medium containing freshly dispersed NPs. Cells were exposed to NPs (OC-Fe_3O_4 and U-Fe_3O_4) in 5 doses: 0.12, 0.6, 3, 15, 75 μg/cm^2, corresponding to 0.57, 2.9, 14, 72, 360 μg/ml NPs (calculated for 6-well plates, 2 ml medium). After 0.5-, 2-, 4- and 24-h treatment, the uptake, comet, TBE and RGA assays were performed.

Human peripheral lymphocytes were collected from blood of 13 volunteers (6 women, 7 men, age 40–50 years). Volunteers participating in the study were not exposed to any known pollutants or mutagens. Blood was collected by venepuncture from fasted subjects and aliquoted in EDTA tubes for the comet assay and in heparinized tubes for measurement of the CBPI and proliferating activity of peripheral blood cells. All study participants signed an informed consent form. This study was approved by the Ethical Committee of the Slovak Medical University in Bratislava. Lymphocytes were isolated by gradient centrifugation. The cell suspension (2×10^6 cells/ml) in RPMI medium was dispensed into a 96-well plate (100 μl/well; growth area 0.32 cm^2). About 25 μl of NP dispersion was added per well with the cell suspension. Cells were treated with 0.12–75 μg/cm^2 NPs for 4 h (in RPMI medium with 10% FBS) and for 24 h (in RPMI medium with 20% FBS). Concentrations used for both NPs are expressed in μg/cm^2 and μg/ml for each test (Table 2).

Tramsmission electron microscopy of cells

TK6 cells in 6-well plates were treated with NPs for 2 h and transferred to 50 ml centrifuge tubes, washed and initially serially fixed in 4% paraformaldehyde (PFA) (10 min) followed by 8%

Table 2. Concentration used for two forms of iron for cell exposure expressed in two dose matrix.

	$U\text{-}Fe_3O_4$, $OC\text{-}Fe_3O_4$	
Method used	$\mu g/cm^2$	$\mu g/ml$
3HTdR	0.12, 3 and 75	0.17, 4.24 and 106
CBPI	3, 15 and 75	5.4, 27 and 135
TBE	0.12, 0.6, 3, 15 and 75	0.57, 2.9, 14.4, 72.0 and 360
RGA	0.12, 0.6, 3, 15 and 75	0.57, 2.9, 14.4, 72.0 and 360
CA PBL	0.12, 0.6, 3, 15 and 75	0.22, 1.13, 5.7, 28.3 and 141
CA TK6	0.12, 0.6, 3, 15 and 75	0.57, 2.9, 14.4, 72.0 and 360

$U\text{-}Fe_3O_4$, uncoated iron oxide; $OC\text{-}Fe_3O_4$, oleate coated iron oxide; ^{3}HTdR, incorporation of ^{3}H thymidine; CBPI, cytochalasin B proliferation index; TBE, trypan blue exclusion; RGA, relative growth activity; CA PBL, the comet assay in peripheral blood lymphocytes; CA TK6, the comet assay in TK6; NPs, nanoparticles.

PFA (20 min, 4 °C). Cells were then collected in a microcentrifuge tube, and centrifuged ($500 \times g$, 10 min; $100 \times g$, 2 min; $2000 \times g$, 2 min; $4000 \times g$, 2 min; $8000 \times g$, 2 min; $12\,000 \times g$, 5 min). The supernatant was replaced with 1% PFA, and thereafter rinsed 3 times in 0.1 M sodium phosphate buffer (NaPi) (pH 7.4) prior and subsequent to treatment with osmium (0.5% OsO_4 in NaPi for 30–45 min). Samples were then serially dehydrated in 50, 70, 80 and 96% ethanol (15 min) and then in 100% ethanol (3×20 min). Propylene oxide (Sigma-Aldrich) was applied for 2×5 min for further dehydration, before the fixed material was transferred to Durcupan ACM (Sigma-Aldrich) for embedding. After 30 min at 56 °C, the Durcupan was replaced by fresh Durcupan which polymerized for 3–4 h or overnight, at room temperature. Finally, the samples were put in capsuls with Durcupan to polymerize at 56 °C for 48 h.

Ultrathin sections of 90–95 nm were cut using an ultramicrotome (Leica) and transferred to 300 mesh nickel grids. Sections were counterstained with uranyl acetate followed by lead citrate and examined in a TEM (Tecnai 12, FEI). Images were obtained with a Veleta camera.

A suspension of lymphocytes (2×10^6 cells/ml) in RPMI medium with 10% FBS was dispensed into a 96-well plate (200 µl/well; growth area of 0.32 cm^2). Cells were exposed to the NPs at concentrations 0.12–75 $\mu g/cm^2$ for 24 h (in RPMI medium with 10% FBS) and processed for TEM as described above.

Trypan blue exclusion assay

To test for cell membrane integrity (assumed to be a measure of cell viability), TK6 cells were exposed to NPs for 0.5, 2 and 24 h. TK6 cells were disaggregated in the medium after the exposure. About 10 µl of cell suspension was mixed with 10 µl trypan blue (0.4%) and cytotoxicity (percentage of trypan blue-positive cells) was measured using a Countess™ Automated Cell Counter (Invitrogen). Cell viability was determined according to the scheme: TBE (%) = 100 − (number of dead cells/total number of cells counted) × 100.

Relative growth activity of the cells exposed to NPs

TK6 cells exposed to NPs dispersed in fresh medium at a range of doses (0.12, 0.6, 3, 15, 30, 45, 75 $\mu g/cm^2$) were after 48 h disaggregated and counted for their RGA using a Countess™ Automated Cell Counter (Invitrogen). RGA was calculated according to following formula: RGA (%) = (number of cells at day 2/number of cells seeded at day 0) in exposed cultures/(number of cells at day 2/number of cells seeded at day 0) in unexposed control cultures × 100. RGA was expressed graphically.

Proliferative activity of peripheral blood cells: Incorporation of ^{3}H-thymidine into DNA of proliferating cells

About 150 µl of human heparinized whole blood diluted 1:15 in RPMI 1640 (Sigma-Aldrich) medium containing 10% foetal calf serum (FBS, PAA), L-glutamine (Sigma-Aldrich) and gentamycin (Sandoz) was dispensed in triplicate wells of a 96-well microtitre culture plate under sterile conditions. NPs were added in a volume of 25 µl for different exposure intervals (4, 24 h) before the end of the whole 72-h incubation period. The plates were incubated at 37 °C and 5% CO_2 for 48 h; then wells were pulsed with 1 µCi ^{3}H-thymidine (^{3}H-TdR; Moravek) diluted in 20 µl medium and incubated at 37 °C for a further 24 h. After incubation, cell cultures were harvested onto glass fibre filter paper. Filters were placed in scintillation fluid (Perkin Elmer) and radioactivity was measured using a Beta Scintillation counter Microbeta 2 (Perkin Elmer). Counts per minute (cpm)/per culture were measured in triplicate for each variable.

The cytokinesis-block proliferation index

CBPI was analyzed as a part of the CBMN assay as described previously in Tulinska et al. (2015). Cultures were set up in duplicate by adding 0.5 ml whole blood to 4.5 ml of RPMI medium with L-glutamine and $NaHCO_3$ (Sigma) supplemented with 10% FBS and antibiotics (penicillin and streptomycin, Gibco) in 9 cm^2 flasks and treated with NPs (3, 15 or 75 $\mu g/cm^2$) for 24 h. Culture medium with NPs was discarded by centrifugation ($90 \times g$ for 10 min) and cells were resuspended in fresh culture medium prepared and supplemented with 0.18 mg/ml PHA to stimulate lymphocytes for 72 h at 37 °C. Cytochalasin B (Sigma, 6 µg/ml) was added for the last 28 h to accumulate cells that had completed one nuclear division at the binucleated stage (Fenech, 2007). After the incubation period, cells were hypotonically treated in 0.075 M KCl and fixed twice with methanol/glacial acetic acid, 3:1. The fixed cells were dropped onto slides; air dried and stained with 2% Giemsa-Romanowski solution for 10 min. CBPI was determined on 500 cells. CBPI was calculated as [no. of mononucleated cells (MNCs) + 2 × no. of binucleated cells (BNCs) + 3 × no. of multinucleate cells] total no. of cells. These measurements were used to estimate cytotoxicity by comparing values in the treated and control cultures. Scoring criteria for selection of MNCs, and BNCs corresponded to those of the HUMN project (http://www.humn.org). Untreated negative control cells and positive control cells treated with mitomycin C (0.05 µg/ml) for 24 h were assayed in parallel cultures. Treatment of cultures with cytochalasin B, and measurement of the relative frequencies of MNCs, BNCs and multinucleated cells in the culture, provide an accurate method of quantifying the effect on cell proliferation and the cytotoxic or cytostatic activity of a treatment and ensure that only cells that divided during or after treatment are scored.

The alkaline comet assay for detection of single and double strand breaks and oxidized purines

TK6 cells and peripheral blood mononuclear cells (lymphocytes) after exposure were resuspended and aliquoted into microcentrifuge tubes. In the case of TK6 cells, 5×10^3 cells were embedded in 120 µl of 1% low melting point (LMP) agarose in PBS at 37 °C. About 5 µl drops of the mixture in parallel for each sample were placed on a glass microscope slide (precoated with melted 0.5% normal melting point agarose in H_2O) using a 12 gel format template for positioning 12 gels per slide. Peripheral lymphocytes suspended in LMP agarose (2×10^4 cells in 45 µl of mixture) were immediately pipetted onto a microscope

slide and covered with 15 mm × 15 mm coverslip. Three agarose gels were placed per slide. The slides were consequently placed for 5 min at 4 °C to solidify, coverslips removed and slides immersed in lysis solution (2.5 M NaCl, 0.1 M EDTA, 10 mM Tris–HCl, pH 10 and 1% Triton X-100 added immediately before use) for 1–24 h at 4 °C. During the lysis cell membranes, cytoplasm and most chromatin proteins are removed, leaving the free nuclear DNA in the agarose gel. For FPG enzyme treatment, slides were washed 3 times for 5 min in cold (4 °C) FPG enzyme reaction buffer (40 mM HEPES, 0.1 M KCl, 0.5 mM EDTA, 0.2 mg/ml bovine serum albumin, pH adjusted to 8.0 with KOH) in a staining jar. About 30 µl of FPG in buffer (final dilution – 1/3000) or reaction buffer alone (as a negative control) was added to the gel, and covered with a cut piece of Parafilm. Slides were incubated in a moist box for 30 min at 37 °C, put for 5 min at 4 °C and Parafilm removed. FPG was provided by Department of Nutrition, University of Oslo, Norway. After lysis or enzyme incubation, slides were placed on the platform in a horizontal electrophoresis tank, immersed in cold (4 °C) electrophoresis solution (0.3 M NaOH; 1 mM EDTA) for 20 min and subjected to electrophoresis at 25 V (0.8 V/cm, ~300 mA) for 20 min. After neutralization for 10 min in PBS, followed by 10 min in water, slides were dried at room temperature. Samples were stained with 2000 × diluted SYBR Gold (Invitrogen) in TE buffer (10 mM Tris–HCl, 1 mM EDTA, pH 7.5–8.0), covered with a cover slip and viewed by fluorescence microscopy (Leica DMI 6000 B for TK6 cells, Olympus BX40F4 for lymphocytes) and CCD camera. Quantification was done using image analysis system Comet assay IV (Perceptive Instruments Ltd.), scoring 100 comets per sample. As positive controls, cells were treated with 50 µM H_2O_2 in PBS (4 °C) for 5 min on ice.

Statistical analysis

For the comet assay, Student's *t*-test was used for statistical analysis. Data are presented as mean values ± SD. *p* values indicating statistically significant results are shown thus; $*p<0.05$; $**p<0.01$; $***p<0.001$.

For CBPI and proliferative activity tests SPSS 16.0 software was used for statistical analysis. Normality was tested by Shapiro–Wilcoxon's test. To test for significant differences between groups the independent samples *T*-test (or paired-samples *T*-test) for normally distributed data, and the Mann–Whitney *U*-test (or Wilcoxon test) for non-normally distributed data were used. Differences between three groups were tested by one-way analysis of variance (ANOVA) and by Bonferroni's test if equal variances were assumed or by Tamhane's test if equal variances were not assumed. The Kruskall–Wallis test was used for non-normally distributed data. The data were expressed as mean values with standard deviation (means ± SD) or standard error of mean (means ± SEM). Differences at $p<0.05$ were considered to be statistically significant.

Results

NP characterization

Suspensions of OC-Fe_3O_4 and U-Fe_3O_4 NPs were characterized in terms of physical and chemical properties. Specific characterization was devoted to the determination of impurities of potential toxicological concern. TEM observations (Figure 1) confirmed the declared data about size and size distribution, while AAS and ICP-OES confirmed the high purity of the provided NPs. HPLC-MS confirmed that the oleic acid was added as sodium oleate, which was partly freely dissolved (960 ppm) in the original dispersion, while the remaining oleate was coating the particles.

In order to estimate the specific surface area of OC-Fe_3O_4 and U-Fe_3O_4 NPs, different procedures had to be applied. The best procedure for estimation of specific surface area of U-Fe_3O_4 NPs dispersion was a very slow evaporation at room temperature of water before pre-treatment under N_2 flow. This procedure could not be applied to the OC-Fe_3O_4 NP dispersion since the oleate would coat the particles during the evaporation process, getting misleading results. The ''single point'' BET technique was applied. TEM analyses confirmed similar surface area of OC-Fe_3O_4 NPs and U-Fe_3O_4.

By Zero Field Cooling/Field Cooling (ZFC/FC) measurement (Binns et al., 2002), we determined the intrinsic magnetic behaviour of OC-Fe_3O_4 NPs to be superparamagnetic, while U-Fe_3O_4 NPs exhibit only paramagnetic behaviour. Knowing that the particles in the dispersions are the same, and taking into account their concentrations in the dispersions, such different magnetic behaviour can be attributed to the presence of oleate, which prevents particle-particle interactions and enhances superparamagnetic behaviour, which is not the case in the uncoated dispersion due to agglomeration effects.

Cytotoxicity of U-Fe_3O_4 and OC-Fe_3O_4 NPs

The cytotoxic potential of U-Fe_3O_4 NPs and OC-Fe_3O_4 NPs as well as of sodium oleate was investigated *in vitro* in human lymphoblastoid TK6 cells and in peripheral blood lymphocytes. The cells were exposed to both coated and uncoated Fe_3O_4 NPs at concentrations of 0.12–75 µg/cm^2. Cytotoxicity in TK6 cells was measured by relative growth activity (RGA) assay, measuring cellular growth activity (cell death or reduction of proliferation activity and prolongation of generation time). The trypan blue exclusion (TBE) assay of membrane integrity was used as a viability check on TK6 cells after NP exposure at all time points. Cytotoxicity in lymphocytes was measured by CBPI and by incorporation of ^{3}H-TdR into DNA of proliferating blood cells.

U-Fe_3O_4 NPs did not inhibit RGA of TK6 cells at any of the concentrations tested, and was thus found not to be cytotoxic (Figure 2). Consistent with this, no effect on cell membrane integrity was observed by TBE assay at any time point investigated (Figure 2). In primary lymphocyte cultures, U-Fe_3O_4 NPs did not decrease the CBPI index at any of the tested concentrations and time points compared to negative control (Figure 3). No significant change in proliferation activity was detected with the ^{3}H-TdR incorporation assay in lymphocytes at concentrations not interfering with the assay (Figure 3). The decrease in proliferation activity of lymphocytes treated at 15 and 75 µg/cm^2 of U-Fe_3O_4 NPs for 4 h and at 75 µg/cm^2 for 24 h was attributed to interference with the assay (Figure 4). Thus, also in lymphocytes, U-Fe_3O_4 NPs were not found to exert cytotoxicity.

OC-Fe_3O_4 NPs induced high cytotoxicity in the RGA assay, where the number of (viable) cells able to proliferate decreased to 7.5% at 30 µg/cm^2. Induction of cytotoxicity was found to be dose-dependent (Figure 5). The TBE assay showed slightly reduced cell viability, of TK6 cells at 45 µg/cm^2 (76% after 0.5 h; 66% after 2 h) whereas 75 µg/cm^2 strongly decreased cell viability (42.5% after 0.5 h; 48% after 2 h). The effect was found to be dose-dependent also in this assay (Figure 5). After 24 h exposure of TK6 cells to OC-Fe_3O_4 NPs, viability was significantly decreased (down to 51%) from a concentration of 30 µg/cm^2 OC-Fe_3O_4 NPs.

In human peripheral blood cells, OC-Fe_3O_4 NPs were found to interfere with the assay. Thus the apparent greatly decreased proliferation at 75 µg/cm^2 after both 4 and 24 h of exposure can be attributed in part to the interference of NPs with the assay

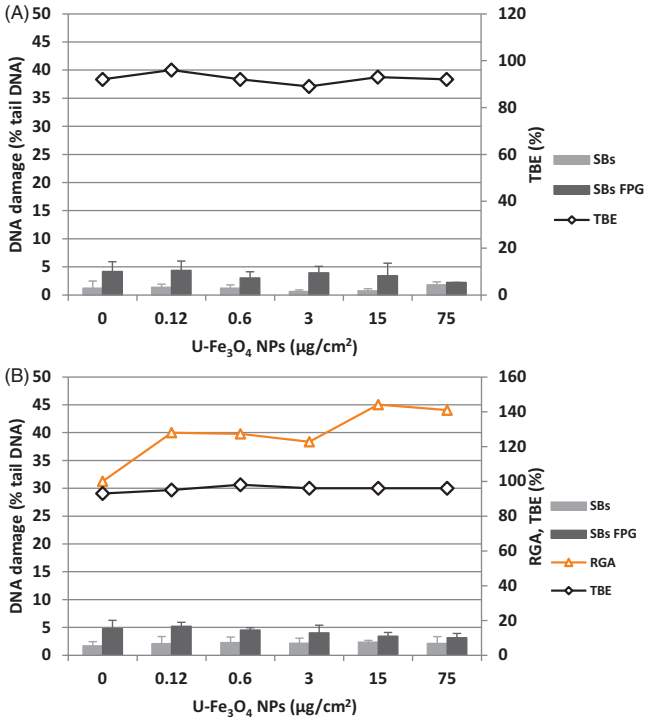

Figure 2. Cytotoxicity and genotoxicity of uncoated (U-Fe_3O_4) NPs in TK6 cells. DNA damage (strand breaks and oxidized purines) measured by the Comet assay (CA) modified with FPG, and cytotoxicity measured by trypan blue exclusion assay (TBE) and relative growth activity assay (RGA) in TK6 cells exposed to U-Fe_3O_4 NPs after (A) 2-h exposure time and (B) 24-h exposure time. DNA damage is expressed as strand breaks (SBs) and strand breaks with FPG-sensitive sites (SBs + FPG) – representing altered purines. Data are presented as mean values ± SD.

(Figures 3 and 4). However, the highest dose (75 µg/cm^2) of OC-Fe_3O_4 NPs seemed to be cytotoxic also for peripheral blood cells (Figure 3). On the other hand, we observed no significant changes of the CBPI index after OC-Fe_3O_4 NP treatment in the concentration range 3–75 µg/cm^2 (for 24 h) compared to negative control (Figure 3). The positive control, MMC (0.05 µg/ml) significantly decreased CBPI. Thus, in human peripheral blood cells, OC-Fe_3O_4 NPs were found to be cytotoxic according to the ^{3}H-TdR incorporation assay, and this was found also for TK6 cells by RGA and TBE assays; however, cytotoxicity was not detected with the CBPI assay.

A possible cytotoxic effect of sodium oleate (used as coating) was investigated in TK6 cells with the RGA assay (Figure 6). The cells were treated with sodium oleate at concentrations of 10.8, 21.6 or 108 µg/ml. The lowest concentration (10.8 µg/ml) correlates with the amount of sodium oleate present in the highest applied OC-Fe_3O_4 NP concentration (75 µg/cm^2). This concentration did not decrease RGA or viability, and was thus found not to be cytotoxic itself. The same negative result was found for 21.6 µg/ml of sodium oleate (corresponding to 2× the concentration applied in 75 µg/cm^2 of OC-Fe_3O_4 NPs). However, a cytotoxic effect was found only at the highest concentration (108 µg/ml) of sodium oleate tested, which corresponds to 10× the concentration of sodium oleate present in the 75 µg/cm^2 OC-Fe_3O_4 NPs (Figure 6). Thus introduction of oleate surface coating of Fe_3O_4 NPs changed the features and cytotoxic potential of the otherwise not very toxic Fe_3O_4 NPs. The induced toxicity was not due to intrinsic toxicity of oleate.

Cellular uptake of NPs and cell morphology of exposed TK6 and human peripheral blood cells: evaluation by transmission electron microscopy

Consistent with the cytotoxicity data, investigations by TEM of embedded cells revealed highly damaged cells among the primary blood cells (data not shown) as well as the TK6 cells in the OC-Fe_3O_4 NPs treated group (Figure 7G–J). Control cells seemed viable with intact membranes (Figure 7 A–B).

TK6 cells surrounded by OC-Fe_3O_4 NP clusters tended to be dead or dying. In these cells, NP clusters were found both along the plasma membrane, the nuclear membrane and membranes of intracellular organelles or vacuoles in cells with lysed plasma membrane. Cells that were not completely surrounded by OC-Fe_3O_4 NPs appeared healthy and viable. Often highly necrotic cells were seen next to viable cells with intact membranes. The effect was dose-dependent, as augmented damage and more dying cells were detected at the highest concentration. Relatively few NPs were detected intracellularly in cells with intact membranes. Here the NPs were detected in nucleus, vacuoles, mitochondria as well as in cytoplasm (Figure 7G–J).

U-Fe_3O_4 NP-treated TK6 and blood cells showed a different pattern. The NPs tended to cluster in large networks extracellularly and did not cluster along the membranes as OC-Fe_3O_4 NPs were found to. The cells had intact membranes and seemed viable, consistent with the cytotoxicity data. However, intracellular vacuoles were seen in many of the cells, indicating that cells were affected (Figure 7C–F).

Uptake of U-Fe_3O_4 NPs into most of monocytes and lymphocytes was found already after exposure to 3 µg/cm^2. Cells had condensed chromatin, and were heavily vacuolized. NPs were found mostly in vacuoles, and rarely in the nucleus. Other cell subpopulations (erythroblasts, erythrocytes, neutrophils) were undamaged (data not shown).

Genotoxicity of U-Fe_3O_4 NPs, OC-Fe_3O_4 NPs and oleate: detection of DNA strand breaks and oxidized DNA lesions by the comet assay

The alkaline comet assay with and without lesion-specific glycosylase FPG was used to measure the DNA-damaging potential of U-Fe_3O_4 NPs, OC-Fe_3O_4 NPs and sodium oleate in TK6 cells and in isolated human peripheral lymphocytes. DNA damage is expressed as strand breaks (SBs) and oxidized DNA lesions (FPG-sensitive sites representing altered purines) together with SBs (SBs + FPG). H_2O_2 was used as positive control for SBs (average value 20.5% tail intensity in TK6 cells and 25.1% in human peripheral lymphocytes).

The results with TK6 and human peripheral lymphocytes were consistent for both coated and uncoated NPs, though the effect seemed more pronounced in human lymphocytes. While U-Fe_3O_4 NPs did not induce DNA damage in the applied concentration range (Figures 2 and 8), OC-Fe_3O_4 NPs induced DNA damage in both TK6 cells (exposure up to 2 h) (Figure 5) as well as at all tested conditions for blood lymphocytes (Figure 9). A significant slight increase in DNA damage compared to negative control was observed at non-cytotoxic concentrations (15 and 30 µg/cm^2 after 0.5-h exposure, and 3 and 30 µg/cm^2 after 2-h exposure) of OC-Fe_3O_4 NPs, indicating genotoxicity. Induction of strand breaks was time- and dose-dependent. An increase in SBs + FPG sites representing overall DNA oxidation was observed after 0.5 h, and in both SBs and SBs + FPG sites after 2-h exposure at 45 µg/cm^2 of OC-Fe_3O_4 NPs. At this concentration a slightly (25%) reduced cell viability was observed. After 0.5 - and 2-h exposure of TK6 cells with the highest concentration (75 µg/cm^2) of OC-Fe_3O_4 NPs, a high level of SBs and SBs + FPG sites was found (Figure 5), most likely as a result of high cytotoxicity (~50%).

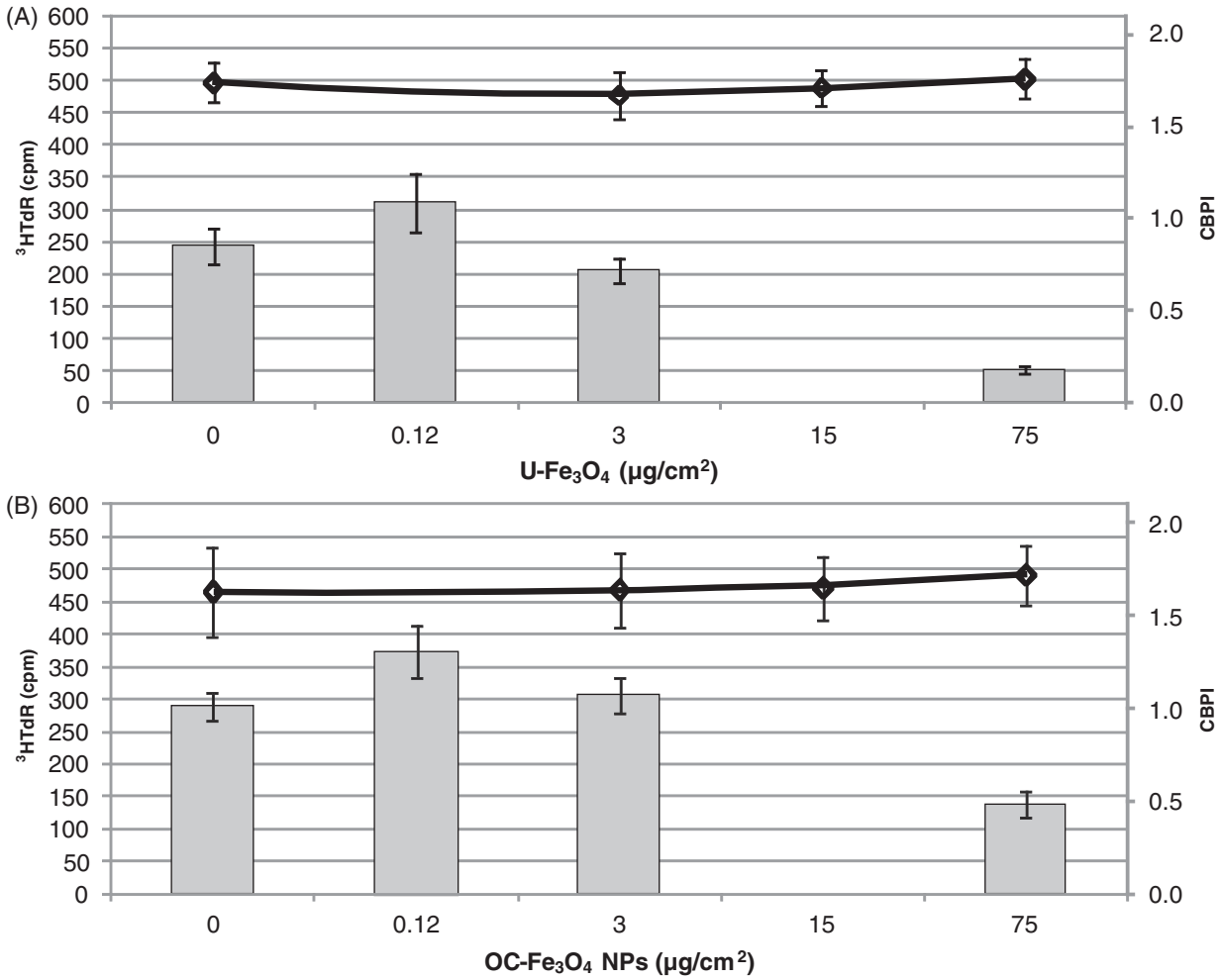

Figure 3. Cytotoxicity of peripheral blood cells. Cytotoxicity was measured as Cytokinesis block proliferation index (CBPI) and Proliferative activity (PA) measured as incorporation of ^{3}H-TdR into DNA of proliferating peripheral blood lymphocytes of human volunteers after cellular exposure to uncoated (U-Fe_3O_4) (A) and coated (OC-Fe_3O_4) iron oxide NPs (0.12, 3, 15 and 75 µg/cm^2) for 24 h. The CBPI data are presented as means ± SD. Mitomycin C (0.05 µg/ml) was used as a positive control. For PA, the bars show means ± SEM. Cyclophosphamide (40 mg/ml) was used as suppressive control.

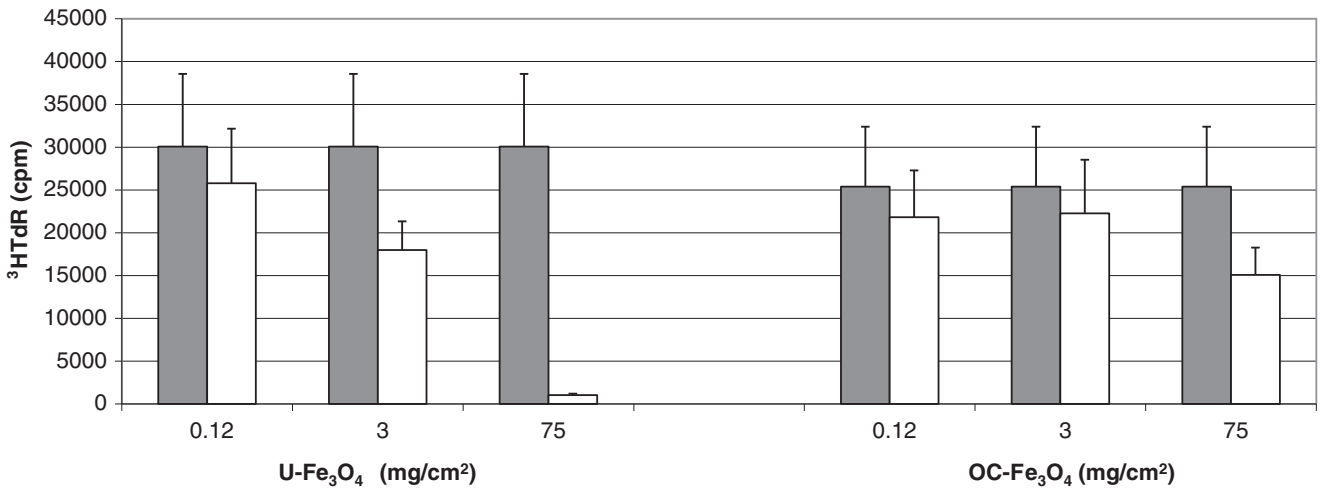

Figure 4. Interference of NPs with the proliferation assay. Proliferative activity of peripheral blood cells was measured as incorporation of ^{3}H-TdR into replicating cells. Results are expressed as cpm – counts/minute/culture, and presented as mean + SEM. The blood cells were isolated from human volunteers ($n = 4$). Grey bars indicate cultures treated with mitogen phytohaemagglutinin A. White bars represent corresponding cultures where NPs were added immediately before harvesting the cells.

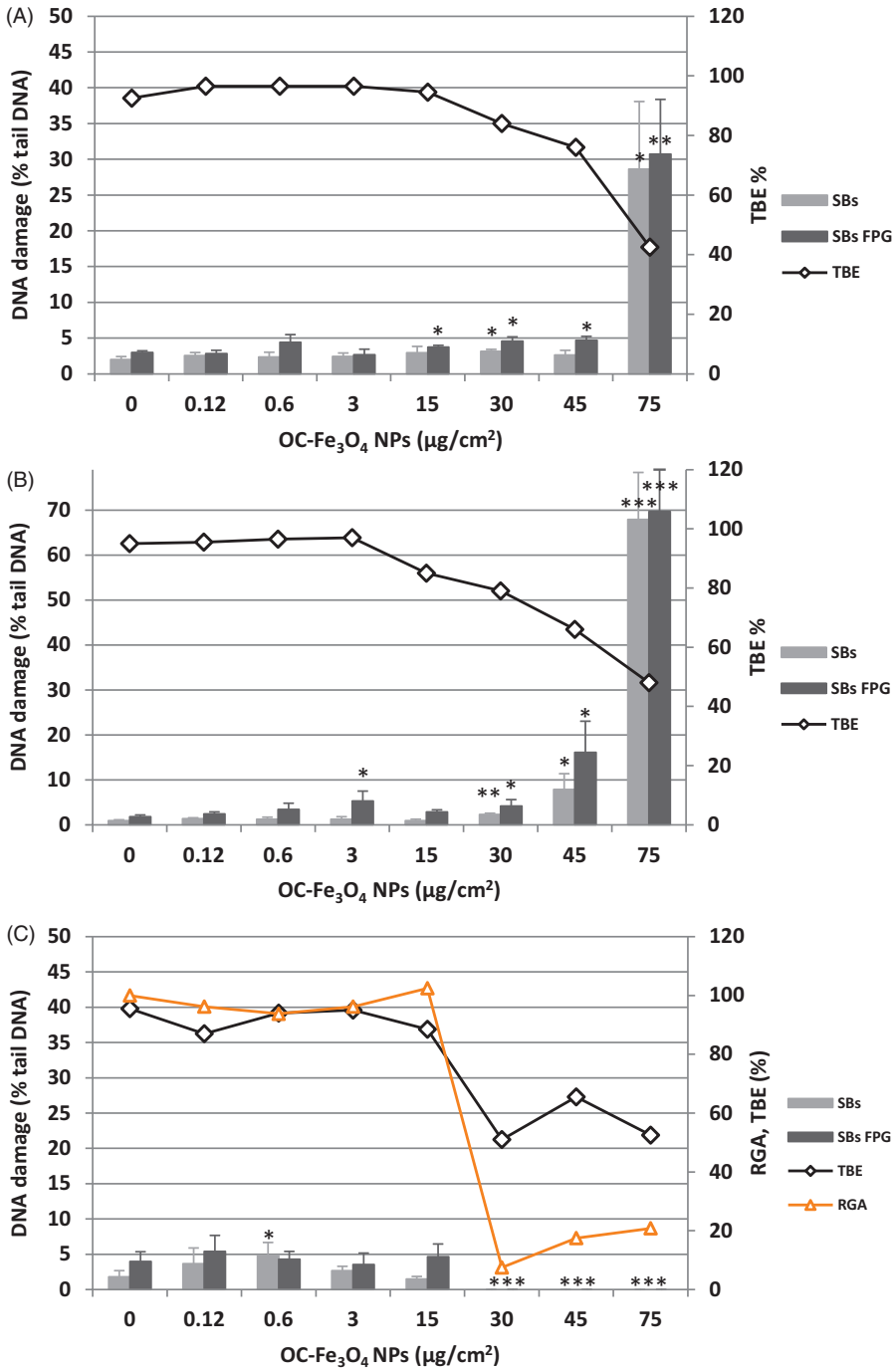

Figure 5. Cytotoxicity and genotoxicity of coated (OC-Fe_3O_4) NPs in TK6 cells. Comet assay (CA) modified with FPG, trypan blue exclusion assay (TBE) and relative growth activity assay (RGA) on TK6 cells exposed to coated (OC-Fe_3O_4) iron oxide NPs after (A) 0.5 h exposure time, (B) 2 h exposure time and (C) 24 h exposure time. DNA damage expressed as strand breaks (SBs) and strand breaks with FPG-sensitive sites (SBs + FPG) – representing altered purines. Data are presented as mean values ± SD. p Values indicate statistically significant results; *$p < 0.05$; **$p < 0.01$; ***$p < 0.001$.

Due to high cytotoxicity observed in TK6 cells after long exposure time (24 h) with OC-Fe_3O_4 NPs in the higher concentrations (from 30 to 75 µg/cm^2), it was not possible to measure DNA damage as no comets were found (due to excessive DNA fragmentation). Hence longer exposure (24 h) of TK6 with OC-Fe_3O_4 NPs was only found to induce genotoxicity at one non-cytotoxic concentration (0.6 µg/cm^2) (Figure 5).

In peripheral human blood lymphocytes exposure to 15 µg/cm^2 of OC-Fe_3O_4 NPs for 4 h induced significant genotoxic response, i.e. increase of SBs and SBs + FPG compared to non-exposed control (Figure 9). The level of SBs and SBs + FPG sites increased with exposure time (Figure 9). After 4 h of exposure to non-cytotoxic concentrations (3 and 7.5 µg/cm^2), we found significant increase of SBs. After 24-h exposure, OC-Fe_3O_4 NPs increased the level of SBs (at 7.5 µg/cm^2) and also SBs + FPG sites (3 and 7.5 µg/cm^2). At higher concentrations (30 and 75 µg/cm^2) DNA damage was not measurable due to high cytotoxicity and absence of comets from the gel.

The coating material, sodium oleate, did not increase the levels of SBs or SBs + FPG sites after 24-h exposure at the two lowest concentrations tested (10.8 and 21.6 µg/ml), corresponding to the equal or double concentration of sodium oleate in the highest dose of OC-Fe_3O_4 NPs. The highest sodium oleate concentration tested (108 µg/ml, corresponding to 10× the applied concentration) showed highly damaged DNA due to high cytotoxicity (Figure 6).

Thus, surface coating of Fe_3O_4 NPs with oleate tended to introduce genotoxic features (DNA strand breaks and oxidized base lesions) of the otherwise non-genotoxic Fe_3O_4 NPs. This effect was not due to intrinsic genotoxicity of oleate.

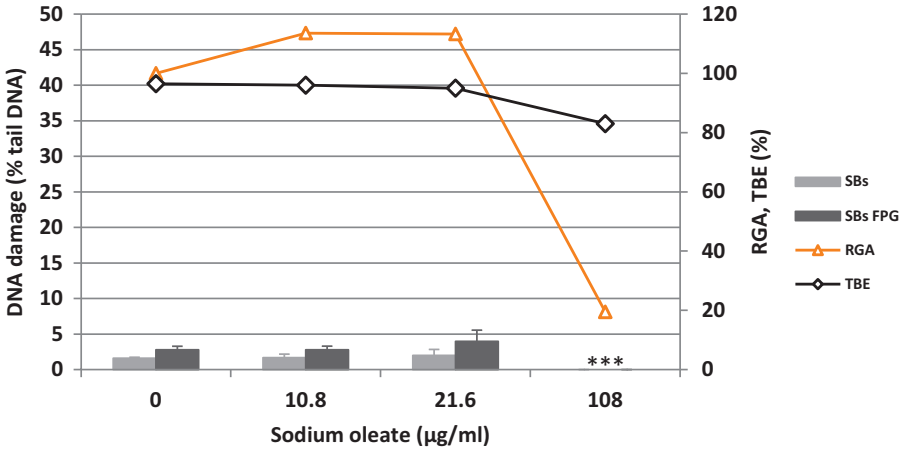

Figure 6. Cytotoxicity and genotoxicity of sodium oleate in TK6 cells. Comet assay (CA) modified with FPG, trypan blue exclusion assay (TBE) and relative growth activity assay (RGA) on TK6 cells exposed to sodium oleate after 24 h. DNA damage expressed as strand breaks (SBs) and strand breaks with FPG-sensitive sites (SBs + FPG) – representing altered purines. Data are presented as mean values ± SD. p Values indicate statistically significant results; $^{***}p < 0.001$.

Discussion

As different coatings (surface modification) of NPs may exhibit different effects on cyto- and genotoxicity (McNeil, 2005), we compared the effects of two types of Fe_3O_4 NPs, uncoated and oleate coated, using cells of blood origin – primary peripheral blood cells – and a human lymphoblastoid cell line, TK6. The two tested types of NPs had the same nominal size (5–12/13 nm), primary particle morphology, purity and surface area (Table 1) and differed only according to whether they were coated or uncoated. Different surface chemistry of NPs can result in different behaviour in solution, as uncoated NPs tend to agglomerate while coated NPs are more dispersed (Ahamed et al., 2008). This is in line with our findings that secondary characteristics in RPMI medium with serum differed between OC-Fe_3O_4 NPs and U-Fe_3O_4 NPs. While OC-Fe_3O_4 NPs were dispersed and formed only nanosized agglomerates, U-Fe_3O_4 formed large microsized agglomerates (Table 1). Therefore, both TK6 cells as well as peripheral blood lymphocytes were cultivated in similar culture media and experimental conditions were otherwise equal to avoid effects induced by different behavior of the NPs in distinct media.

Our cytotoxicity data indicate that introduction of oleate coating of iron oxide NPs, transforms the non-cytotoxic U-Fe_3O_4 NPs into toxic OC-Fe_3O_4 NPs. Cytotoxicity was detected both in TK6 cells and lymphocytes with RGA, TBE and ^{3}H-TdR assays, in contrast to U-Fe_3O_4 NPs which were found to be non-cytotoxic under our experimental set-up. These cytotoxicity data were also supported by TEM analysis. However, by measuring CBPI, we did not detect any cytotoxicity of OC-Fe_3O_4 NPs (nor of U-Fe_3O_4 NPs). The discrepancy between the results of this assay as compared to the three others applied could be accounted for by the distinct endpoints measured, as well as by experimental conditions, such as exposure of cells at different stages of the cell cycle. While in the ^{3}HTdR incorporation assay (peripheral blood cells) as well as in RGA (TK6) cells were exposed in the proliferation phase of cell cycle, in the case of the CBPI assay the peripheral blood cells were exposed before addition of phytohaemagglutinin, i.e. in the G_0 phase phase of the cell cycle. In G_0 phase, the cells are more resistant. Lack of cytotoxicity detected by this assay could also be due to differences in sensitivity between different cell types. However, our results show that the primary peripheral blood cells were more sensitive compared to the stable TK6 cell line. Additionally, proliferating cells without condensed chromatin were more susceptible to exposure to NPs than were non-dividing cells.

Also, the outcome of the proliferation assay can be strongly influenced by interference with incorporation of ^{3}H-TdR, and this effect was clearly higher with U-Fe_3O_4 NPs than with OC-Fe_3O_4 NPs. Thus the slight cytotoxicity detected after exposure to U-Fe_3O_4 NPs in this assay was most likely due to interference with the assay, as no cytotoxicity of U-Fe_3O_4 NPs was detected by any of the other cytotoxicity assays (Guadagnini et al., 2015; Figure 4). This effect could in fact be an interference of metal NPs with liquid scintillation detection of ^{3}H-TdR incorporation. (Figure 4). Thus Fe_3O_4 NPs could be reduced by adsorption of emitted electrons, resulting in diminished excitation of the scintillation fluid and decreased cpm. The apparent diminished ^{3}H-TdR incorporation could also be due to optical quenching of scintillation by Fe_3O_4 (Guadagnini et al., 2015). As TEM analysis of leucocytes exposed for 24 h showed toxic effects of two doses of OC-Fe_3O_4 NPs (3 and 75 µg/cm^2) and a high dose of U-Fe_3O_4 NPs, the discrepancy between CBPI and the ^{3}H-TdR incorporation test cannot be explained solely by interference or differences in cell cycle, but might also be due to different total volumes of complete RPMI medium (5 ml versus 200 µl) used for cell incubation or to a difference in proportion of FBS and human serum. It has also been shown that NPs can interfere with the cell counting devices, such as the automated Countess counting device applied for RGA and TBE. We therefore tested both OC as well as U-Fe_3O_4 and found that the interference of NPs with the Countess was <10% (Guadagnini et al., 2015). OC-Fe_3O_4 agglomerates were recognized by Countess as dead cells and U-Fe_3O_4 as living cells. These results could theoretically lead to slight overestimation of cytotoxicity in the case of OC-Fe_3O_4 and underestimation in U-Fe_3O_4. However, the slight interference with the Countess in our case did not influence our overall results. It is important always to include a control with NPs without cells when counting with the Countess, to check the degree of interference and prevent false positive/negative results. If interference is found, cells should be counted manually (Guadagnini et al., 2015).

Coating of Fe_3O_4 NPs with oleate was found to change the toxic potential of the otherwise non-toxic Fe_3O_4 NPs. However, oleate in itself was not found to be cytotoxic at concentrations correlated with exposed NP concentrations. Thus the oleate coating itself is unlikely to contribute to the toxicity of these NPs. Toxic properties are more likely induced by changes in features of the NPs related to cellular uptake and binding to extracellular receptors or transmembrane channels, as indicated by our TEM analysis. Our results are also in agreement with data obtained by another partner in the NanoTEST project (Kenzaoui et al., 2012a) who found that the same U-Fe_3O_4 NPs were better taken up by human brain-derived endothelial cells (evaluated using Prussian blue reaction as well as by TEM) than were OC-Fe_3O_4 NPs, indicating changes in cellular uptake mechanisms as well as mechanisms for induction of toxicity related to surface modifications and introduction of new characteristics of the NPs in

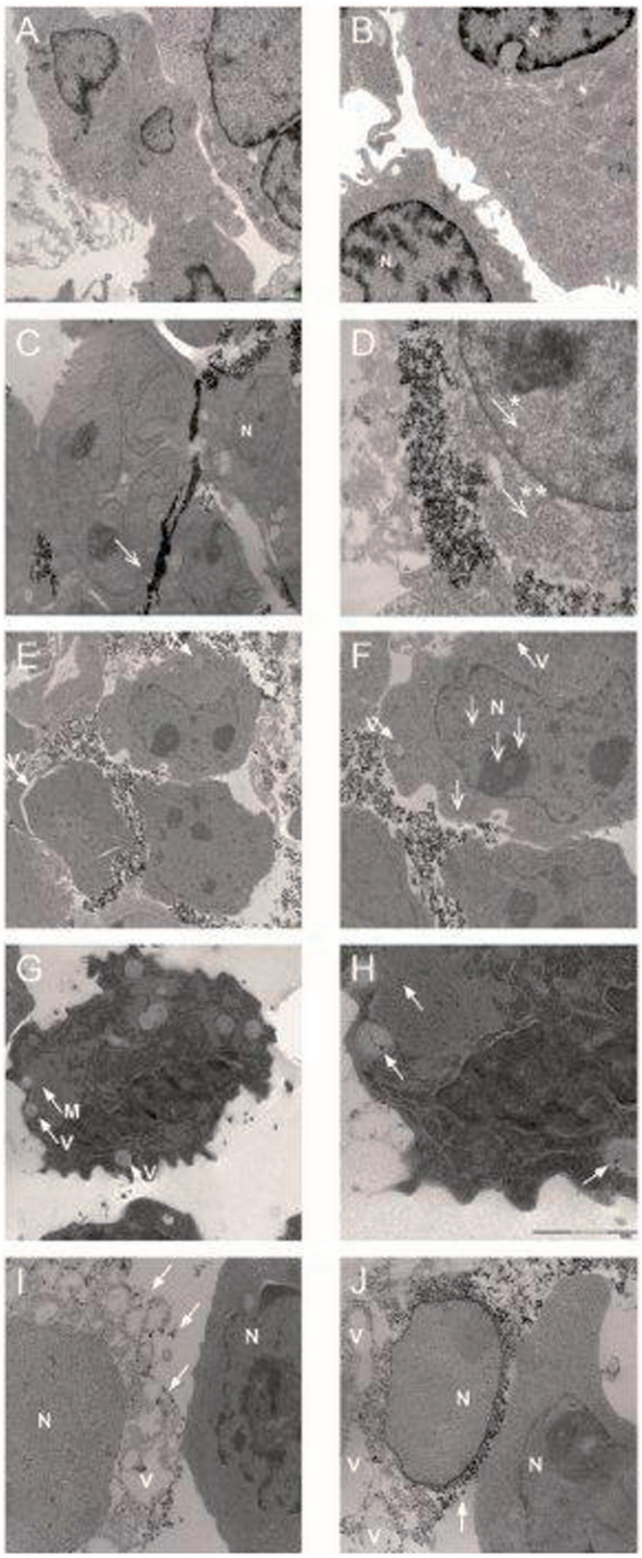

Figure 7. Cellular morphology of TK-6 cells and uptake of iron NPs following exposure to iron NPs, investigated by transmission electron microscopy (TEM). Cellular morphology of untreated TK-6 (control) cells is displayed in figures A and B. TK-6 cells were exposed for 2 h to either uncoated iron oxide NPs at 30 μg/cm^2 (C, D) or 75 μg/cm^2 (E, F), or coated iron oxide NPs at 30 μg/cm^2 (G and H) or 75 μg/cm^2 (I and J). Coated particles induced higher cellular damage (G–J) than uncoated, in spite of the greater uptake of uncoated NPs (C–F). NPs that entered cells were seen in the nucleus (N), but also in cytoplasm where formations of vacuoles (V) were seen at certain concentrations. NPs were also observed in the mitochondria (M) (F). Sizes of NPs were roughly estimated to be about 7.3 nm (D,*) and about 14.6 nm (D,**).

dispersion. OC-Fe_3O_4 NPs were poorly taken up by cells but displayed cytotoxicity at concentrations >100 μg iron/ml, while U-Fe_3O_4 NPs exhibited greater cellular uptake but did not show cytotoxicity up to 200 μg iron/ml. The extent of uptake might depend on the surface charge of NPs (Kenzaoui et al., 2012a). While OC-Fe_3O_4 NPs are negatively charged, U-Fe_3O_4 NPs are close to neutral (Table 1). Moreover, uptake of negatively charged OC-Fe_3O_4 NPs by human colon cells was much lower than uptake of positively charged polyvinylamine coated Fe_3O_4 NPs (Kenzaoui et al., 2012b). Also, the agglomeration state influenced uptake, as U-Fe_3O_4 was taken up into cells to a larger extent than was OC-Fe_3O_4. In TK6 cells, we found NPs in cytoplasm, vacuoles, mitochondria and nucleus (Figure 7). In blood cells, U-Fe_3O_4 was taken up by monocytes and lymphocytes but not by erythroblasts, erythrocytes or neutrophils. In both cell types, blood cells as well as TK6 cellular uptake of OC-Fe_3O_4 was relatively low, although cells were clearly dead or dying.

It seems that the state of aggregation/agglomeration is another important feature that influences both behaviour of NPs and toxic outcome. In our previous study with TiO_2 NPs (Magdolenova et al., 2012a), cytotoxic and genotoxic effects were found to depend on the state of aggregation. While better dispersed NPs forming agglomerates in the nanosize range did not cause cytotoxicity and genotoxicity, TiO_2 dispersed in medium without serum formed larger agglomerates and induced DNA damage (SBs and oxidized DNA lesions) in three cell lines including TK6 (Magdolenova et al., 2012a). In general, smaller NPs are considered to be more toxic because they can more easily enter the cell. However, in our study as well as in that of Kenzaoui et al. (2012a,b), uptake of agglomerated U-Fe_3O_4 NPs was higher than uptake of dispersed OC-Fe_3O_4 NPs. As large agglomerates are not stable, it is also possible that smaller nanosized agglomerates or individual NPs are being released and as such reach the cells. In addition, large aggregates could mechanically damage the cell and also deform the nucleus on entry into the cell (Di Virgilio et al., 2010). In our study, however, larger agglomerates did not seem to damage the cell membrane. U-Fe_3O_4 NPs were taken up by the cells as small agglomerates or individual NPs and were found also in the nucleus. However, they did not induce cytotoxicity or DNA damage and genotoxicity.

Clearly coating influenced behaviour of NPs, as OC-Fe_3O_4 NPs were more toxic and also induced DNA damage in both cell cultures. NPs invasively surrounded individual cells, attaching along the cell membranes and consequently causing cell death. Different surface properties of the tested NPs also attract molecules from surrounded medium, especially proteins, thus forming a protein corona (Monopoli et al., 2011).

Our TEM data indicate that OC-Fe_3O_4 NPs do not need to enter the cells to induce toxicity. Rather it seems that the NPs are exerting an extracellular stimulus, e.g. by modifications of transmembrane receptors or channels, an effect transformed into a cellular response by coupling to intracellular cell death signalling pathways.

In spite of the internalization of U-Fe_3O_4 NPs by cells and localization in nucleus, using the comet assay we did not observe any significant increase in the level of strand breaks or DNA oxidation after exposure to these NPs in either TK6 cells or lymphocytes. In contrast, exposure of TK6 cells to OC-Fe_3O_4 NPs led to DNA damage even though these NPs were poorly taken up by cells. The comet assay is one of the most promising methods for genotoxicity testing, including testing of nanomaterials, due to its simplicity, versatility, and the ability to detect different DNA lesions; it is the most used assay to evaluate potential genotoxicity of NPs (reviewed by Magdolenova et al., 2014). In our study, we applied the alkaline comet assay to examine DNA strand breaks and used lesion-specific glycosylase FPG to evaluate

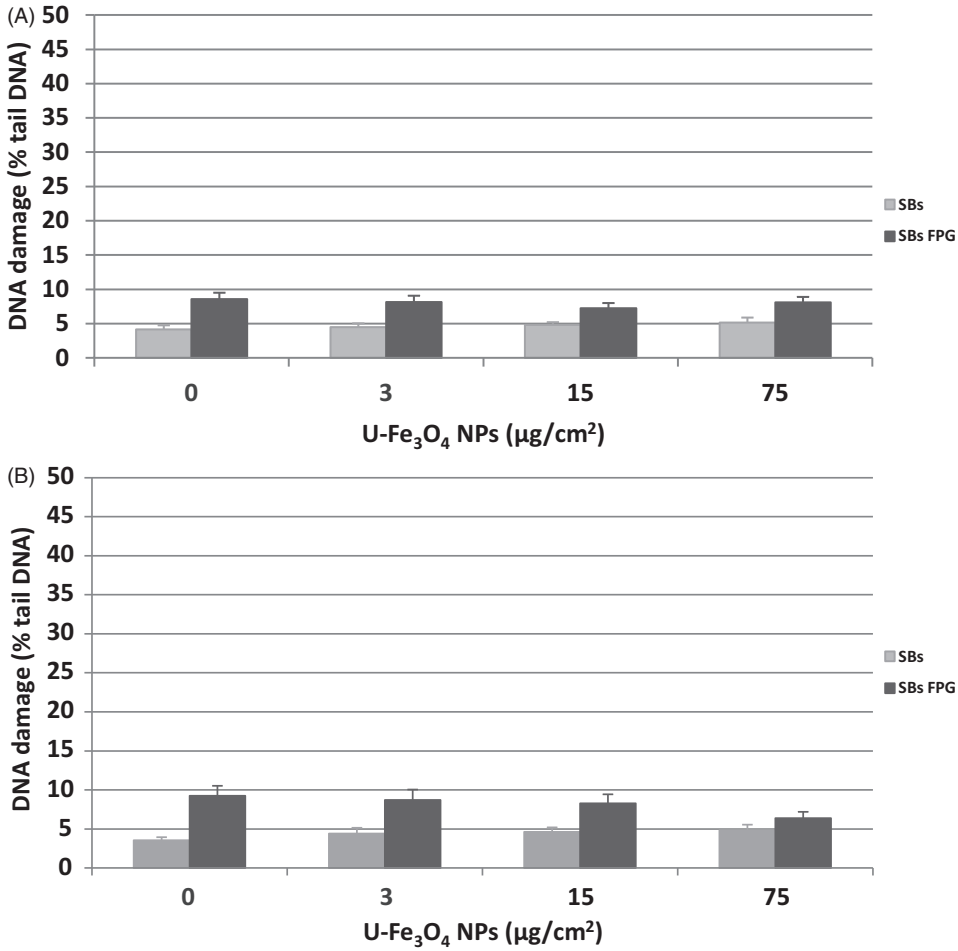

Figure 8. Genotoxicity of uncoated (U-Fe_3O_4) NPs in human peripheral blood lymphocytes. Comet assay (CA) modified with FPG on human peripheral blood lymphocytes exposed to uncoated (U-Fe_3O_4 NPs) nanomagnetite after (A) 4 h, (B) 24 h DNA damage was expressed as strand breaks (SBs) and strand breaks with FPG-sensitive sites (SBs + FPG) – representing altered purines. Data are presented as mean values ± SD.

oxidative damage to DNA in cells treated with both U-Fe_3O_4 and OC-Fe_3O_4 NPs. Some studies report an interference of the comet assay with NPs (Karlsson, 2010; Stone et al., 2009), especially with FPG (Kain et al., 2012). However, we tested several NPs, including both types of Fe_3O_4 NPs, and did not find any interference (Magdolenova et al., 2012b).

We observed time- and concentration-dependent responses in both TK6 cells and lymphocytes. DNA damage was found at both cytotoxic (30–75 µg/cm^2) as well as non-cytotoxic concentrations, the latter clearly indicating genotoxicity. The DNA damage observed at highly toxic doses cannot be ascribed to genotoxicity. With the comet assay it is important to combine cytotoxicity and genotoxicity measurements of NPs, as cells with low viability usually exhibit high levels of SBs and DNA oxidation. To prevent false positive interpretation of genotoxic response, a non-toxic/slightly toxic concentration scale needs to be employed (Magdolenova et al., 2014; Olive & Banáth, 1995). In our study, we set the limit for non-cytotoxic dose as a 20% decrease in RGA for each exposure time compared to non-exposed negative control. The dose giving a genotoxic effect was inversely related to the time of exposure (starting with 30 µg/cm^2 after 0.5 h up to 0.6 µg/cm^2 of OC-Fe_3O_4 NPs after 24 h). The DNA-damaging potential of OC-Fe_3O_4 NPs was low, but statistically significant. By using TK6 cells and lymphocytes as a blood model of NP exposure, we obtained similar results on genotoxicity of both forms of Fe_3O_4 NPs. This indicates that TK6 cells provide a good representative model for blood, even though peripheral human lymphocytes exhibited higher sensitivity. Our results are in agreement with those obtained on Cos-1 and Balb/3T3 cells showing greater cytotoxic effects of OC-Fe_3O_4 NPs than U-Fe_3O_4 NPs (Harris et al., 2015). However, the pH2Ax assay did not detect any DSBs in Balb/3T3 cells after exposure to both Fe_3O_4 NPs at non-cytotoxic concentrations. Only a low level of DNA damage (detected by the comet assay) was found in Cos-1 after 2-h exposure to non-cytotoxic concentrations of OC-Fe_3O_4 NPs; this might be explained by lower sensitivity of kidney and embryonic fibroblast cells to DNA damage, in comparison with the presently used blood cells.

Conclusions

Oleate coating of Fe_3O_4 NPs changed the behaviour, toxicity and internalization of the NPs, as well as inducing pathological morphological changes in the cells. OC-Fe_3O_4 NPs were found to be both cytotoxic and genotoxic, in contrast to U-Fe_3O_4 NPs. However, it is questionable which properties are responsible for induction of toxicity by OC-Fe_3O_4, as neither the oleate coating nor Fe_3O_4 NPs themselves were found to be toxic in primary blood cells or a cell line of blood origin. Oleate coating changed properties of Fe_3O_4 NPs in terms of surface charge and agglomeration potential. In contrast to U-Fe_3O_4 NPs, OC-Fe_3O_4 NPs were negatively charged and stably dispersed in the medium. The different charge might cause difference in interactions with other compounds present in medium, such as serum proteins,

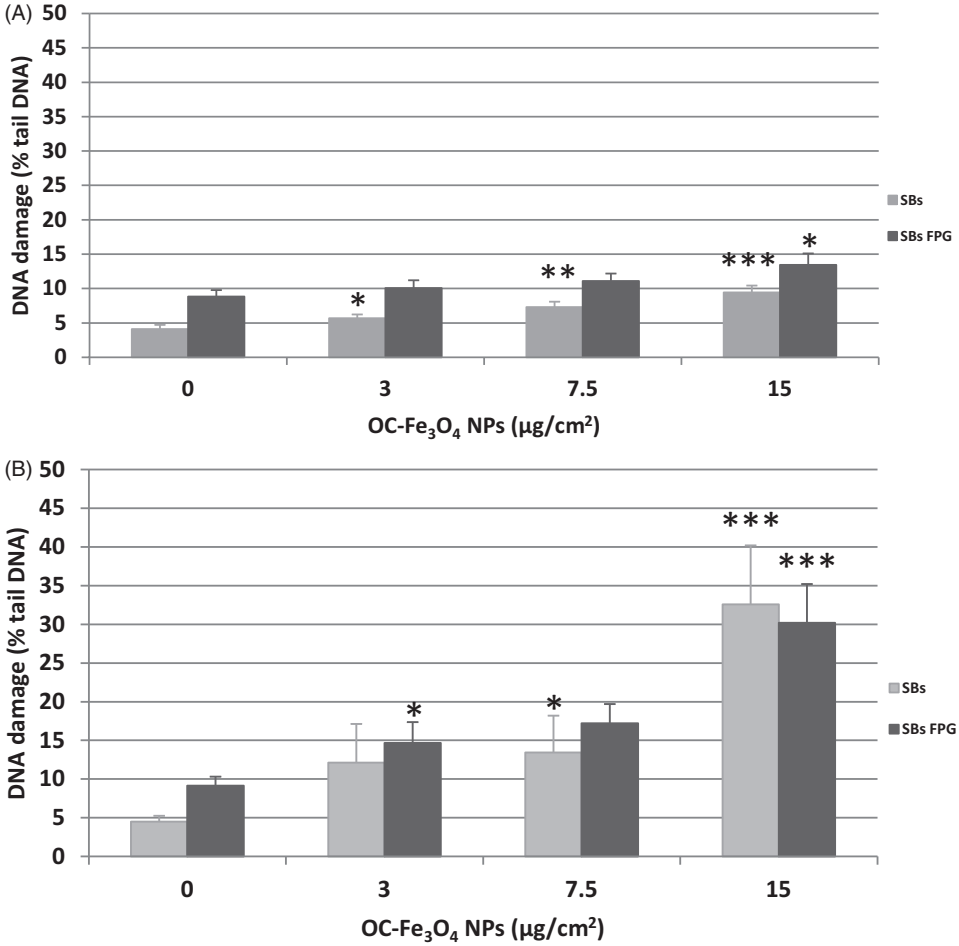

Figure 9. Genotoxicity of coated (OC-Fe_3O_4) NPs in human peripheral blood lymphocytes. Comet assay (CA) modified with FPG on human peripheral blood lymphocytes exposed to coated (OC-Fe_3O_4NPs) iron oxide after (A) 4-h exposure time and (B) 24-h exposure time. DNA damage expressed as strand breaks (SBs) and strand breaks with FPG-sensitive sites (SBs + FPG) – representing altered purines. Data are presented as mean values ± SD. *p* Values indicate statistically significant results; *$p < 0.05$; **$p < 0.01$; ***$p < 0.001$.

as well as with cell membranes, and thus could have impact on internalization of NPs and toxicity. Unlike U-Fe_3O_4, OC-Fe_3O_4 NPs narrowly surrounded the cell membrane. Cellular uptake was low for both types of NPs, and only OC-Fe_3O_4 NPs induced cytotoxicity and genotoxicity. Our data show that OC-Fe_3O_4 NPs do not need to enter the cells to induce a toxic response, but are more likely to act via extracellular stimulation of intracellular cell death signalling pathways.

Acknowledgements

The authors would also like to thank D. Cristofori and V. Trevisan (Department of Molecular Sciences and Nanosystems; University Ca' Foscari Venice, Italy), F. Spizzo (Department of Physics, University of Ferrara, Italy), H. Nagyova, E. Mrvikova and K. Gavalova (Slovak Medical University, Bratislava, Slovakia) and F. Bjørklid (NILU, Kjeller, Norway) for their technical support during characterization of the nanomaterials and TEM images. We also are grateful for brilliant assistance with preparation of sections for electron microscopy analysis by Jorunn Knutsen and Bjørg Riber, TEM expertise offered by B. Hakim and access to TEM facilities at Department of Anatomy, University of Oslo, Norway.

Declaration of interest

The authors declare that there is no conflict of interest. The work was supported by EC FP7 NanoTEST [Health-2007-1.3-4], Contract no: 201335, EC FP7 QualityNano [INFRA-2010-1.131], Contract No: 214547-2, EC FP7 NANoREG, [NMP.2012.1.3-3] contract no: 310584, by the ITMS project no. 2424012033, Operational research and development program financed from the European Regional Development Fund and by NILU internal projects 106179 and 106170.

References

Ahamed M, Karns M, Goodson M, Rowe J, Hussain SM, Schlager JJ, Hong Y. 2008. DNA damage response to different surface chemistry of silver nanoparticles in mammalian cells. Toxicol Appl Pharmacol 233: 404–10.

Auffan M, Decome L, Rose J, Orsiere T, De Meo M, Briois V, et al. 2006. In vitro interactions between DMSA-coated maghemite nanoparticles and human fibroblasts: a physicochemical and cyto-genotoxical study. Environ Sci Technol 40:4367–73.

Berry CC, Wells S, Charles S, Aitchison G, Curtis AS. 2004. Cell response to dextran-derivatised iron oxide nanoparticles post internalisation. Biomaterials 25:5405–13.

Binns C, Maher MJ, Pankhurst QA, Kechrakos D, Trohidou KN. 2002. Magnetic behavior of nanostructured films assembled from preformed Fe clusters embedded in Ag. Phys Rev B 66:184413;1–12.

Brunauer S, Emmett P, Teller E. 1938. Adsorption of gases in multimolecular layers. J Am Chem Soc 60:309–19.

Cengelli F, Maysinger D, Tschudi-Monnet F, Montet X, Corot C, Petri-Fink A, et al. 2006. Interaction of functionalized superparamagnetic iron oxide nanoparticles with brain structures. J Pharmacol Exp Ther 318:108–16.

Di Virgilio AL, Reigosa M, Arnal PM, Fernández Lorenzo de Mele M. 2010. Comparative study of the cytotoxic and genotoxic effects of

titanium oxide and aluminium oxide nanoparticles in Chinese hamster ovary (CHO-K1) cells. J Hazard Mater 177:711–8.
Fenech M. 2007. Cytokinesis-block micronucleus cytome assay. Nat Protoc 2:1084–104.
Guadagnini R, Halamoda Kenzaoui B, Cartwright L, Pojana G, Magdolenova Z, Bilanicova D, et al. 2015. Toxicity screenings of nanomaterials: challenges due to interference with assay processes and components of classic in vitro tests. Nanotoxicology 9(S1):13–24.
Guardia P, Batlle-Brugal B, Roca AG, Iglesias O, Morales MP, Serna CJ, et al. 2007. Surfactant effects in monodisperse magnetite nanoparticles of controlled size. J Magn Magn Mater 316:756–9.
Harris G, Palosaari T, Magdolenova Z, Mennecozzi M, Gineste JM, Saavedra L, et al. 2015. Iron oxide nanoparticle toxicity testing using high throughput analysis and high content imaging. Nanotoxicology 9(S1):87–94.
Jain TK, Richey J, Strand M, Leslie-Pelecky DL, Flask CA, Labhasetwar V. 2008. Magnetic nanoparticles with dual functional properties: drug delivery and magnetic resonance imaging. Biomaterials 29:4012–21.
Kain J, Karlsson HL, Möller L. 2012. DNA damage induced by micro- and nanoparticles – interaction with FPG influences the detection of DNA oxidation in the comet assay. Mutagenesis 27:491–500.
Karlsson HL. 2010. The comet assay in nanotoxicology research. Anal Bioanal Chem 398:651–66.
Karlsson HL, Cronholm P, Gustafsson J, Möller L. 2008. Copper oxide nanoparticles are highly toxic: a comparison between metal oxide nanoparticles and carbon nanotubes. Chem Res Toxicol 21:1726–32.
Karlsson HL, Gustafsson J, Cronholm P, Möller L. 2009. Size-dependent toxicity of metal oxide particles – a comparison between nano- and micrometer size. Toxicol Lett 188:112–8.
Kenzaoui BH, Bernasconi CC, Hofmann H, Juillerat-Jeanneret L. 2012a. Evaluation of uptake and transport of ultrasmall superparamagnetic iron oxide nanoparticles by human brain-derived endothelial cells. Nanomedicine 7:39–53.
Kenzaoui BH, Vilà MR, Miquel JM, Cengelli F, Juillerat-Jeanneret L. 2012b. Evaluation of uptake and transport of cationic and anionic ultrasmall iron oxide nanoparticles by human colon cells. Int J Nanomedicine 7:1275–86.
Kim EH, Ahn Y, Lee HS. 2007. Biomedical applications of superparamagnetic iron oxide nanoparticles encapsulated within chitosan. J Alloys Compd 434/435:633–6.
Magdolenova Z, Bilaničová D, Pojana G, Fjellsbø LM, Hudecova A, Hasplova K, et al. 2012a. Impact of agglomeration and different dispersions of titanium dioxide nanoparticles on the human related in vitro cytotoxicity and genotoxicity. J Environ Monit 14:455–64.
Magdolenova Z, Lorenzo Y, Collins A, Dusinska M. 2012b. Can standard genotoxicity tests be applied to nanoparticles? J Toxicol Environ Health A 75:800–6.
Magdolenova Z, Collins A, Kumar A, Dhawan A, Stone V, Dusinska M. 2014. Mechanisms of genotoxicity. A review of in vitro and in vivo studies with engineered nanoparticles. Nanotoxicology 8:233–278.
McNeil SE. 2005. Nanotechnology for the biologist. J Leukoc Biol 78: 585–94.
Monopoli MP, Walczyk D, Lowry-Campbell A, Elia G, Lynch I, Baldelli Bombelli F, Dawson KA. 2011. Physical-chemical aspects of protein corona: relevance to in vitro and in vivo biological impacts of nanoparticles. J Am Chem Soc 133:2525–34.
Olive PL, Banáth JP. 1995. Sizing highly fragmented DNA in individual apoptotic cells using the comet assay and a DNA crosslinking agent. Exp Cell Res 221:19–26.
Schütz CA, Juillerat-Jeanneret L, Mueller H, Lynch I, Riediker M; NanoImpactNet Consortium. 2013a. Therapeutic nanoparticles in clinics and under clinical evaluation. Nanomedicine 8:449–67.
Schütz CA, Juillerat-Jeanneret L, Soltmann C, Mueller H. 2013b. Toxicity data of therapeutic nanoparticles in patent documents. World Patent Information 35:110–14.
Stone V, Johnston H, Schins RP. 2009. Development of in vitro systems for nanotoxicology: methodological considerations. Crit Rev Toxicol 39:613–26.
Taupitz M, Schmitz S, Hamm B. 2003. Superparamagnetic iron oxide particles: current state and future development. Rofo 175:752–65.
Tulinska J, Kazimirova A, Kuricova M, Barancokova M, Liskova A, Neubauerova E, et al. 2015. Immunotoxicity and genotoxicity testing of PLGA-PEO nanoparticles in human blood cell model. Nanotoxicology 9(S1):33–43.
Wu W, Chen B, Cheng J, Wang J, Xu W, Liu L, et al. 2010. Biocompatibility of Fe3O4/DNR magnetic nanoparticles in the treatment of hematologic malignancies. Int J Nanomedicine 5:1079–84.
Yin H, Casey PS, McCall MJ, Fenech M. 2010. Effects of surface chemistry on cytotoxicity, genotoxicity, and the generation of reactive oxygen species induced by ZnO nanoparticles. 21. Langmuir 26: 15399–408.
Yin H, Too HP, Chow GM. 2005. The effects of particle size and surface coating on the cytotoxicity of nickel ferrite. Biomaterials 26:5818–26.
Ying E, Hwang HM. 2010. In vitro evaluation of the cytotoxicity of iron oxide nanoparticles with different coatings and different sizes in A3 human T lymphocytes. Sci Total Environ 408:4475–81.
Zhang L, He R, Gu HC. 2006. Oleic acid coating on the monodisperse magnetite nanoparticles. Appl Surf Sci 253:2611–17.